Science of the Total Environment 746 (2020) 141186

Contents lists available at ScienceDirect

Science of the Total Environment

journal homepage: www.elsevier.com/locate/scitotenv

Short Communication

A simple, inexpensive method for gas-phase singlet oxygen generation from sensitizer-impregnated filters: Potential application to bacteria/virus inactivation and pollutant degradation

Michael Oluwatoyin Sunday [a,b], Hiroshi Sakugawa [a,*]

[a] Graduate School of Biosphere Science, Hiroshima University, 1-7-1, Kagamiyama, Higashi-Hiroshima 739-8521, Japan
[b] Department of Chemistry, Federal University of Technology, P.M.B. 704, Akure, Ondo State, Nigeria

HIGHLIGHTS

- Gas-phase singlet oxygen ($^1O_2$) generation from Rose Bengal-impregnated filter
- A simple experimental set-up for gas phase $^1O_2$ estimation from impregnated filter
- Sensitizer loading and light intensity were the most important factors.
- Potential application of $^1O_2$ for indoor bacteria/virus inactivation in air

GRAPHICAL ABSTRACT

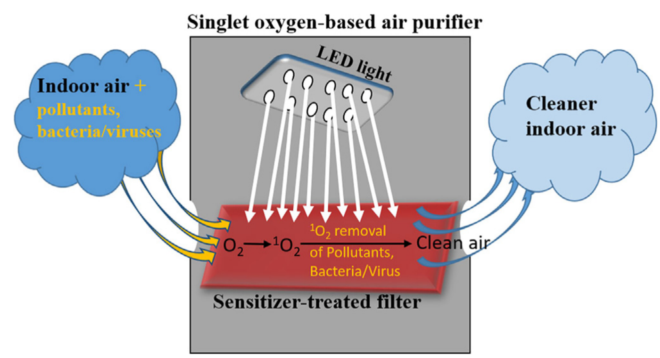

ARTICLE INFO

Article history:
Received 30 April 2020
Received in revised form 26 June 2020
Accepted 21 July 2020
Available online 23 July 2020

Editor: Prof. Pavlos Kassomenos

Keywords:
Singlet oxygen
Indoor air pollution
Bacteria/virus inactivation
Air purifier
Rose Bengal
Membrane filter

ABSTRACT

Airborne infectious diseases such as the new Coronavirus 2019 (COVID-19) pose serious threat to human health. Indoor air pollution is a problem of global environmental concern as well. Singlet oxygen ($^1O_2$) is a reactive oxygen species that plays important role in bacteria/virus inactivation and pollutant degradation. In this study, we found that commercially available filters typically deployed in air purifier and air conditioning units, when impregnated with Rose Bengal (RB) as a $^1O_2$ sensitizer, can be used for heterogeneous gas-phase generation of $^1O_2$. It was confirmed that irradiation of the RB filter under oxygen gas stream produced $^1O_2$, which was measured using furfuryl alcohol trapping method followed by HPLC analysis. It was also observed that the amount of $^1O_2$ generated increases as the light intensity increased. Similarly, the sensitizer loading also positively influenced the $^1O_2$ generation. The heterogeneous gas-phase generation of $^1O_2$ can find potential applications in air purifier and air conditioning units for the purpose of bacteria/virus inactivation and/or pollutant degradation thereby improving indoor air quality.

1. Introduction

Air pollution is a problem of global concern, with indoor air pollution particularly worrisome. Indoor air can be polluted with both chemical and microbial contaminants thereby posing a great threat to human health. The outbreak of airborne infectious diseases such as the recent Coronavirus disease (COVID-19) requires methods for virus inactivation in indoor air. SARS-CoV-2 (the virus responsible for COVID-19) remained viable in aerosols for up to 3 h under environmental conditions (van Doremalen et al., 2020). Therefore, poor ventilation may enable the spread when infected and uninfected people are in close

* Corresponding author.
E-mail address: hsakuga@hiroshima-u.ac.jp (H. Sakugawa).

https://doi.org/10.1016/j.scitotenv.2020.141186
0048-9697/

contact or in a closed environment. The involvement of reactive oxygen species (ROS) such as singlet oxygen ($^1O_2$) in bacteria/virus inactivation and pollutant degradation can be explored for the purpose of improved indoor air quality.

Singlet oxygen, which is molecular oxygen in its lowest excited electronic state, is a reactive oxygen species (ROS) that is photochemically formed by the action of an irradiation light on a photosensitizer in the presence of molecular oxygen. It is involved in the degradation of pollutants (Latch et al., 2003; Liu & Sun, 2011; Kim et al., 2012; Xie et al., 2018; Blacha-Grzechnik et al., 2020) and inactivation of bacteria/virus (Banks et al., 1985; Dahl et al., 1987, 1988; Lenard et al., 1993; Nitzan et al., 1995; Wainwright et al., 1998; Usacheva et al., 2001; Villen et al., 2006; Bartusik et al., 2012a; Costa et al., 2012; Felgenträger et al., 2014; Kim et al., 2020). Photodynamic inactivation (PDI), which involves generating ROS such as $^1O_2$ upon irradiation of a sensitizer, has been deployed to inactivate a wide range of bacteria and viruses. PDI occurs via two mechanisms, namely: Type I mechanism involving the generation of free radicals, and Type II mechanisms involving $^1O_2$. Type II mechanism involving generation of $^1O_2$ has been shown to be the predominant mechanism of bacteria/virus inactivation (Costa et al., 2012). Comprehensive reviews highlighting the various bacteria (Hamblin and Hasan, 2004; Liu et al., 2015) and viruses (Costa et al., 2012) inactivated by $^1O_2$ are available in literature. Viruses including human immunodeficiency virus (HIV), influenza virus, Sendai virus (Lenard et al., 1993), dengue virus (Huang et al., 2004), vaccinia virus (Turner and Kaplan, 1968), adenovirus (Schagen et al., 1999), enterovirus (Wong et al., 2010) etc. have all been reported to be inactivated by $^1O_2$. In addition, it was showed that herpesvirus and influenza virus (enveloped type) and adenovirus and poliovirus (unenveloped type) were inactivated by $^1O_2$ using a spray of Rose Bengal (RB) solution as mist and air scavenging system (Masaoka et al., 2013). Furthermore, a recent report by Eickmann et al. (2018) showed that both UVC and methylene blue/light (MB/L) systems were effective in inactivating Ebola virus (EBOV) and Middle East respiratory syndrome coronavirus (MERS-CoV) in blood plasma. The MB/L systems involves irradiation of methylene blue by visible light to produce $^1O_2$. The inactivation of MERS-CoV, which belongs to the same genus and family with Covid-19 virus, suggests that $^1O_2$ may also work for the inactivation of COVID-19 virus.

The above-mentioned reports majorly involved homogeneous $^1O_2$ generation. However, homogeneous generation in aqueous phase cannot be easily deployed to provide $^1O_2$ needed in the gas phase for potential indoor air purification. $^1O_2$ can also be generated from heterogeneous systems where a solid-state sensitizer, either in isolation or deposited by physical and/or chemical modification onto another solid substance, is irradiated in the presence of oxygen gas to generate $^1O_2$, which flows along with the gas stream into a collecting solution where it reacts with a substrate. Reaction of the formed $^1O_2$ with the selective substrate in solution provides evidence of $^1O_2$ generation from the solid-gas heterogeneous system. In addition to substrate solution, involvement of $^1O_2$ in the deactivation of bacteria and viruses in air has also been reported. Kim et al. (2020) showed that $^1O_2$ inactivated micro-organisms in air up to a distance of 10–15 cm away from the source. Several researchers have presented different experimental set-ups based on this heterogeneous system and demonstrated $^1O_2$ generation from them with further application of the generated $^1O_2$ for substrate degradation or bacteria/virus inactivation (Bartusik et al., 2012a, 2012b; Zamadar et al., 2009; Aebisher et al., 2010; Carpenter et al., 2015; Zhao et al., 2014; Hettegger et al., 2015). Nevertheless, the potential application of $^1O_2$ for the purpose of improved air quality has not been well explored. One way of achieving that is to develop products that can generate $^1O_2$ in the gas phase. Such products will help to inactivate micro-organisms in the indoor environment and may find applications as air purifiers in places like small rooms or offices, on automobiles, trains and even hand dryers. This will make a significant contribution towards cleaner indoor air by removing bacteria/virus or pollutants present in the air.

In this study, we present a simple, inexpensive set-up, designed from commonly available materials, for gas-phase $^1O_2$ generation. A filter material typically employed in the air purifier and air conditioning units was impregnated with Rose Bengal and irradiated using a panel of LED lights. Furfuryl alcohol (FFA) in solution was used as a substrate to provide qualitative and quantitative evidence of $^1O_2$ generation from the filter.

2. Materials and methods

2.1. Filter impregnation with Rose Bengal

The reagents and materials used are listed in supplementary information (S1). RB stock was prepared by dissolving 10 g RB in 150 g of the supplied gel. Two pieces of filters of the same dimension (L × W: 7 × 2.2 cm) were cut-out from the same filter material and their initial weights were obtained. RB was physically impregnated into one of the filters by completely immersing it in the RB-dissolved gel for 5 min. The gel was necessary to help impregnate RB in the filter because of the hydrophobic nature of the filter. The other filter was treated with a blank gel and used as the control filter. Both filters were dried overnight using cold air from an air drier. Treating the control filter with the blank gel helped to account for the contribution of the gel to the weight of the filters after drying. The RB-treated filter was further subjected to air blowing to remove any loosely adhered RB particles on the filter. The images of the RB-treated and control filters are presented in Fig. S2. Thereafter, the amount of RB impregnated into the filter was determined gravimetrically from the difference in the weight of the filter before impregnation and weight after impregnation (dry, RB-impregnated filter). The amount of RB per area of filter (mg/ cm^2) was then calculated.

To investigate the effect of sensitizer loading on $^1O_2$ generation, different filters were impregnated with varying amounts of RB. This was done by firstly preparing serial dilutions (10, 50 and 1000-fold dilutions) of the RB stock using the blank gel. Thereafter, filters were treated with these dilute solutions (Fig. S2). The amount of RB impregnated into the filters from treatment with different solutions of RB was also calculated.

2.2. Experimental set-up for $^1O_2$ photogeneration and monitoring

A schematic diagram of the set-up in this study is shown in Fig. 1a while Fig. 1b and c are pictures taken in the dark and during irradiation respectively. The experimental set-up employed involved immersion of the RB-filter, protected by a PTFE hydrophobic filter, in the trapping solution with oxygen flowing through it during irradiation. The RB-impregnated filter was attached to a glass column (length × base i.d.; 8 × 1.3 cm) with an acrylate adhesive. The base of the glass column where the RB-impregnated filter had been attached was then covered by a hydrophobic PTFE filter which was glued to the edges of the glass column and secured tightly to the sides of the column using transparent tapes. The column was stoppered at the top using a silicon stopper with hole. A capillary tube was inserted into the glass column through the hole of the stopper. The tube delivered oxygen gas to the surface of the RB-impregnated filter at a rate of 0.1–0.2 L/min. The stopper ensured that the top of the column was air-tight preventing any loss of oxygen through the top. The stability of this assembly and monitoring potential leakage or damage was ensured by immersing the assembly firstly in ultrapure water for about 5 min prior to immersion in the substrate solution. This preliminary immersion test showed that there was no leakage or leaching of RB into the solution. This rules out any possibility of aqueous phase contribution to $^1O_2$

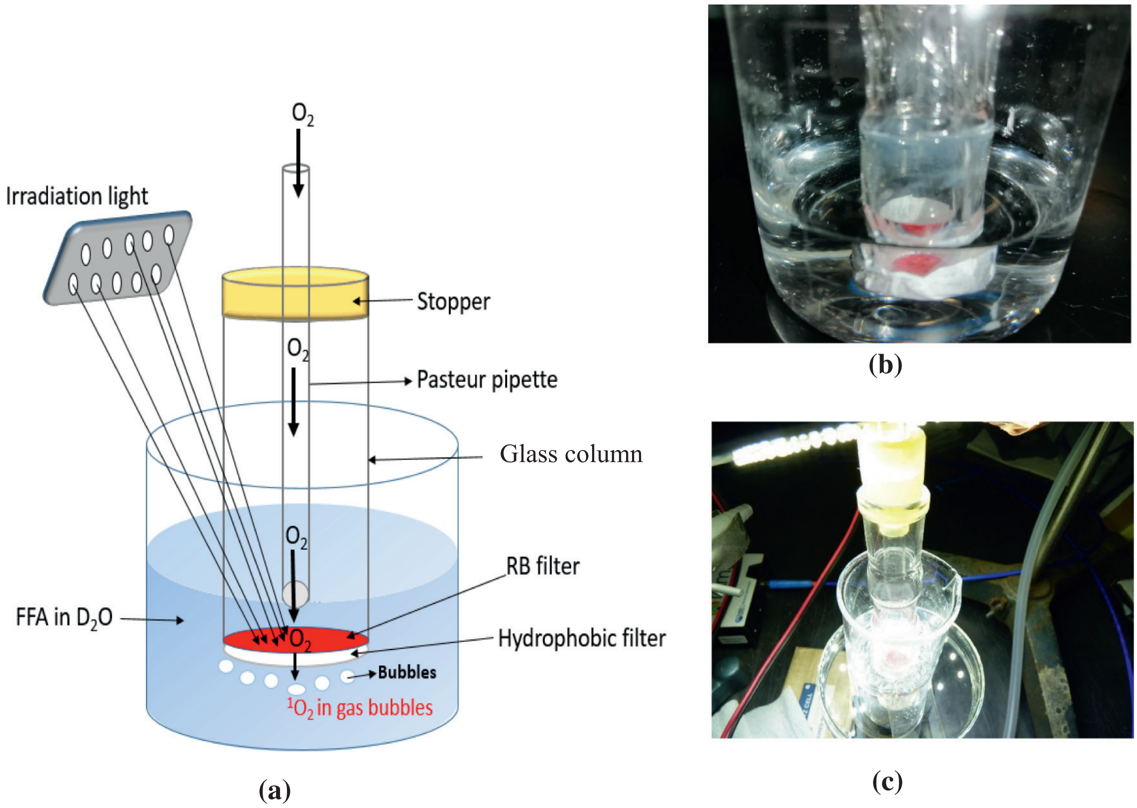

Fig. 1. (a) A schematic diagram of the experimental set-up for $^1O_2$ generation from RB-treated filter. (b) Picture showing the immersion of the assembly in water. This is used to check for potential failure of the assembly, leakage or leaching of RB prior to immersion in the substrate solution and irradiation. (c) Picture of a typical irradiation process for gas-phase $^1O_2$ generation.

generation. The test also showed that at the immersion depth, the gas stream was sufficiently contacting the solution and was not just directly escaping into the air in the laboratory. This was necessary to ensure optimal contact between the $^1O_2$ in the gas stream and the substrate solution. This shows that potential $^1O_2$ exiting the filter along with oxygen flow will contact the reacting solution.

The irradiation light was suspended above the glass column. The light was from a locally fabricated LED panel (Excel Co. Ltd., Fukuyama, Japan) consisting of 60 LED bulbs emitting white light with a power output of up to 144 W when the full irradiation mode is adopted. The spectrum of the irradiation light was obtained using a miniature spectrophotometer device (Flame spectrophotometer, Ocean optics, U.S.A.) while the light intensity was measured using a pyranometer (LI-COR LI-189, U.S.A). As shown in Fig. S1, the LED light has peaks around 445 nm and 550 nm which matches the λ_{max} of RB at about 550 nm.

Four mL solution of 100 μM FFA in D_2O was employed as a substrate to demonstrate $^1O_2$ generation from the irradiation of impregnated filter. $^1O_2$ reacts with FFA to produce 6-hydroxyl-*2H*-pyran-3(*6H*)-one (6-HP-one) as a major product (Haag et al., 1984). $^1O_2$ arriving in the solution was monitored indirectly through the degradation of FFA and corresponding formation of 6-HP-one by HPLC analysis (Supplementary info. S2). Although $^1O_2$ was not generated in solution in this experiment, but in the gas-phase from the irradiation of RB-treated filter, the determined photoformation rate (calculated in solution) is indicative of the amount of $^1O_2$ arriving in the substrate solution. This is expected to be lesser than that generated from the filter due to quenching of some $^1O_2$ as it travels through the pores of the filter, or by the gas stream before successfully contacting the substrate solution. Therefore, the obtained information on $^1O_2$ generation from the filter can be regarded as an estimate.

3. Results and discussion

3.1. Monitoring $^1O_2$ formation

The $^1O_2$ in the oxygen gas stream passing through the filter and arriving in the substrate solution was monitored indirectly by following the peaks of FFA degradation and 6-HP-one formation. Monitoring 6-HP-one formation confirms that the degradation of FFA is due to chemical reaction with $^1O_2$ arriving from the filter into the substrate solution. A typical plot showing the degradation of FFA and corresponding formation of 6-HP-one is shown in Fig. 2a. Furthermore, the degradation of FFA due to $^1O_2$ followed a first order kinetics. The first order plot of FFA degradation during irradiation of RB-treated filter and untreated (blank) filter is shown in Fig. 2b. Irradiation of the RB-treated filter caused a significant degradation of FFA compared to the blank filter. The value obtained for the blank filter was similar to that obtained when the FFA solution was directly irradiated with oxygen flowing into the solution in the absence of the filter assembly. This suggests that the blank filter had no significant contribution to $^1O_2$ formation and that the RB-treated filter was solely responsible for the formed $^1O_2$. In addition, there was no leaching of RB into solution during the irradiation. This is because the hydrophobic PTFE filter shielded the RB-treated filter from directly contacting the solution. This is a very important precaution because RB is highly soluble (100 mg/mL) in water. Therefore, any contact between the RB-treated filter and the solution will encourage a massive leaching or dissolution of RB. Under such scenario, there will be aqueous phase contribution to $^1O_2$ generation. No leaching of RB, in part or whole, was observed during our experiments. This shows that the only source of $^1O_2$ is that generated from the irradiation of the RB-treated filter which reaches the solution through the gas stream. Immersion of the filter assembly, with continuous oxygen flow,

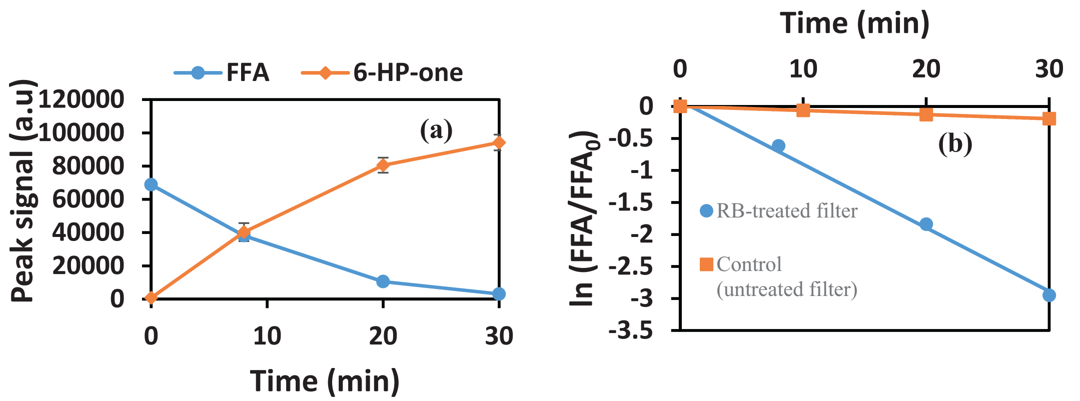

Fig. 2. (a) Degradation of FFA and corresponding formation of 6-HP-one, (b) First order FFA degradation during the irradiation of RB-treated filter. Values are mean of triplicate measurements. Error bars are embedded.

in the dark did not result in any appreciable loss of FFA or formation of 6-HP-one.

3.2. Solvent isotope effect and $^1O_2$ scavenger

The solvent isotope effect and the influence of $^1O_2$ scavengers are two important ways of demonstrating the generation and involvement of $^1O_2$ in a particular reaction. To confirm the presence of $^1O_2$ in the gas stream arriving in the substrate solution, the solvent isotope effect was studied by monitoring the degradation of FFA in D_2O and H_2O under identical experimental conditions using the same RB-treated filter. It is known that $^1O_2$ has a lifetime in D_2O that is about 13 times longer than in water (Lindig et al., 1980). The deactivation rate constant of $^1O_2$ in water is 2.5×10^5 s^{-1}(Rodgers and Snowden, 1982) and 1.6×10^4 s^{-1} in D_2O (Lindig et al., 1980). According to Fig. 3, the degradation of FFA in D_2O was higher than in H_2O. This can be associated with the longer lifetime of $^1O_2$ in D_2O, allowing more $^1O_2$ to undergo chemical reaction with FFA. This confirms the involvement of $^1O_2$ in the degradation of FFA. In the solvent isotope effect, it is important that the concentration of FFA does not contribute significantly to the physical quenching or deactivation of $^1O_2$ in the solvents (D_2O and H_2O). From the product of FFA concentration (100 μM) and the reaction rate constant of $^1O_2$ with FFA (8.3×10^7 M^{-1} s^{-1} in D_2O) (Latch et al., 2003), FFA made a negligible 5% contribution to the deactivation rate constant of 1.6×10^4 s^{-1} for $^1O_2$ in D_2O. Similarly, using the reaction rate constant of 1.09×10^8 M^{-1} s^{-1} (Haag et al., 1984) for the reaction of $^1O_2$ with FFA in H_2O, the 100 μM FFA concentration only made an insignificant 4% contribution to the deactivation rate constant of 2.5×10^5 s^{-1} for $^1O_2$ in H_2O. This shows that the solvent isotope effect is mainly due to collision with the solvents, without any significant contribution from the physical quenching of $^1O_2$ by FFA.

In addition, the effect of $^1O_2$ scavenger on the degradation of FFA in D_2O was studied using NaN_3 as a scavenger. NaN_3 is an efficient scavenger of $^1O_2$ with a second order rate constant of 7.8×10^8 M^{-1} s^{-1} (Wilkinson and Brummer, 1981). The degradation of FFA in D_2O was observed to reduce significantly in the presence of 1 mM NaN_3 compared to its absence (FFA + D_2O, no NaN_3) (Fig. 3). This further confirms the generation of $^1O_2$. The results of the solvent isotope effect and NaN_3 scavenger experiment clearly confirm that $^1O_2$ is present in the gas stream arriving in the substrate solution, and it is responsible for the degradation of FFA.

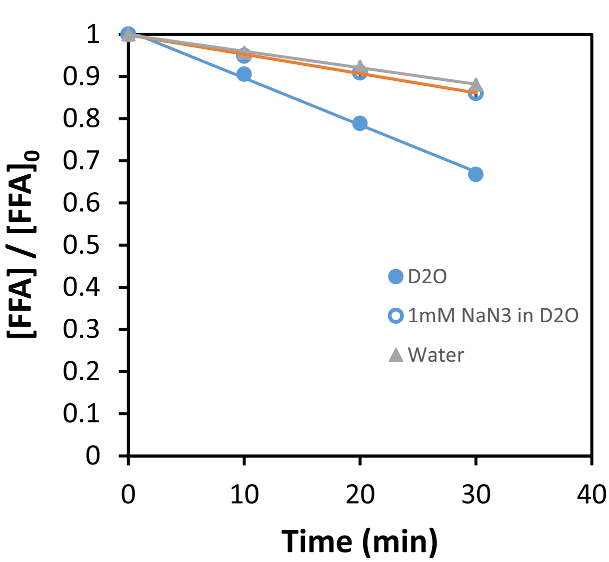

Fig. 3. Effect of solvent and $^1O_2$ scavenger on the reaction of $^1O_2$ with FFA (100 μM). A RB-treated filter was irradiated at an oxygen flow rate of 0.125 L/min. The substrate solution as shown in the figure involve: 100 μM FFA in D_2O, 100 μM FFA + 1 mM NaN_3 in D_2O, 100 μM FFA in water.

3.3. Influence of light intensity

To investigate how light intensity can influence the generation of $^1O_2$, the intensity of the irradiation light was varied by employing the full-power mode and half-power mode of the irradiation light and/or increasing the distance between the filter and irradiation light. A plot of the amount of $^1O_2$ detected in solution, during the irradiation of RB-treated filter, as a function of light intensity is shown in Fig. 4. It is observed that the amount of $^1O_2$ generated increased as the light intensity

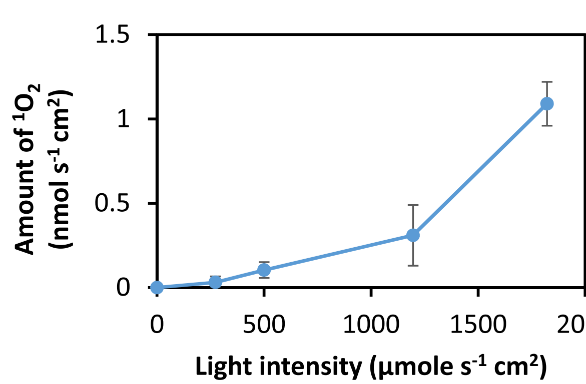

Fig. 4. Effect of light intensity on generation of $^1O_2$. The light intensity values are 0 (dark), 273, 501, 1196 and 1861 μmole s^{-1} cm^2.

increases. The sharp increase between 1196 and 1861 μmole s^{-1} cm^{-2} suggest a regime of light intensity where higher production of $^1O_2$ is observed. Based on the present experimental set-up, the distance between the irradiation light and filter is 11 cm. In an application where the light source is closer to the filter, the light intensity will be much higher and $^1O_2$ generation can be expected to be much higher.

3.4. Effect of amount of sensitizer adsorbed in the filter

The effect of the amount of RB adsorbed by the filter on $^1O_2$ production was investigated by treating blank filters with varying concentrations of RB dissolved in gel. The serial dilutions of the RB stock solution were made by addition of the blank gel to obtain approximately 10, 50 and 1000-fold diluted RB solutions. The rate of $^1O_2$ generation upon irradiation of the filters is shown in Table 1. It is observed that $^1O_2$ generation increased as the amount of RB adsorbed on the filter increased. The maximum solubility of RB in the gel was 10 g RB in 150 g of gel. This was the same solution used as the undiluted stock in Table 1. Therefore, the effect of amount of adsorbed RB on $^1O_2$ generation could not be studied beyond this point. Using the undiluted stock as the highest RB loading possible, the amount of $^1O_2$ reaching the solution was calculated to be 12.8 μmole s^{-1} of $^1O_2$ per mole of RB.

It should be noted that the amount of $^1O_2$ generated on the surface of the filter may be several orders of magnitude higher than the value reported here due to the heterogeneous distribution of $^1O_2$ generation. It has been demonstrated for aqueous solutions that $^1O_2$ generation in the DOM microenvironment could be up to three orders of magnitude higher than in the bulk solution due to physical quenching as the $^1O_2$ diffuses into the bulk solution (Latch & McNeill, 2006; Grandbois et al., 2008). A similar explanation could be adopted here where the $^1O_2$ generated on the surface of the filter may undergo significant quenching before arriving in the substrate solution. This quenching may be caused by the filters (both treated filters and hydrophobic PTFE filter) as the gas stream containing $^1O_2$ migrates from the irradiated side of the filter to the substrate solution. Also, quenching by ground-state molecular oxygen may also arise. Therefore, the quantity of singlet oxygen reported here can only be considered as a minimum. Nevertheless, in the real applications, the filters will be directly exposed to light, while air is circulated or brought into contact with the filter. Under such circumstances, the amount of generated on the surface of the filter is $>>$ than $^1O_2$ migrating further away from the filter into the air. Therefore, contaminated air will encounter a large amount of $^1O_2$ on the surface of the filter that will be significant towards bacteria/virus inactivation.

4. Conclusions

$^1O_2$ generation from the irradiation of a sensitizer-impregnated filter was successfully demonstrated in this study using simple, inexpensive laboratory and commercially-available materials. By using filters already deployed in air purifier and air conditioner units for this study, we have successfully demonstrated that $^1O_2$-generating ability can be incorporated into impregnated filters. Such filters can find potential application for bacteria/virus inactivation in indoor environment by incorporating them into air purifiers. Current commercially available purifiers make use of ozone (O_3) or hydroxyl radical (•OH) in their systems. Ozone is harmful to health. Also, some ozone-based purifiers have been shown to increase the background indoor ozone level. Consequently, the use of O_3, especially in indoor environments has been discouraged. The •OH-based systems generate •OH by the high energy UVC irradiation (185 nm) of water vapor using UVC lamps containing mercury (Crosley et al., 2017) or by heterogeneous photocatalytic oxidation technology (Zhong and Haghighat, 2015). The disposal of such lamps constitutes an environmental concern and they pose health threats if carelessly handled by unsuspecting users. Also, the mechanisms of •OH generation also produces O_3 (Crosley et al., 2017) which may increase the O_3 levels in the indoor environment. Singlet oxygen-based purifiers as proposed in this study present a number of advantages. Firstly, the involvement of $^1O_2$ in the inactivation of a wide range of bacteria and viruses has been well documented in literature (Banks et al., 1985; Lenard et al., 1993; Wainwright et al., 1998; Villen et al., 2006; Bartusik et al., 2012; Costa et al., 2012; Felgenträger et al., 2014; Kim et al., 2020). Similar evidence for •OH is insufficient. Therefore, $^1O_2$-based air purifiers can potentially provide protection against a wider range of bacteria and viruses. Secondly, the lifetime in air is about 85 ms (Schweitzer and Schmidt, 2003) while that of •OH ranges between 0.01 and 1 s (Crosley et al., 2017). The lifetimes of both •OH and $^1O_2$ may be lower depending on the nature of other substances present. Hence, these values can be considered to be their upper limit values at ground-levels in the atmosphere. Nevertheless, the use of RB as sensitizer, which has a high $^1O_2$ quantum yield (0.76) (Wilkinson et al., 1992), can ensure relatively high production of $^1O_2$. Therefore, more $^1O_2$ can be available for bacteria/virus inactivation in $^1O_2$-based air purifiers compared to •OH in •OH-based systems. In addition, the system proposed in this study makes use of simple, cheap and commercially-available LED light sources emitting white light in the visible region, in-line with the λ_{max} of RB (550 nm). Such light source is relatively simple, easier to handle and maintain. The findings from this study can contribute significantly to the development of $^1O_2$-based air purifiers with potential applications in small or large indoor environments in offices, at homes or even on automobiles and trains. Such products are necessary to contribute to improved indoor air quality considering the outbreak of airborne viral infections such as the present COVID-19. Although this is a preliminary study, the findings from this study have led to the development of a prototype where additional parameters necessary for its deployment are being studied.

Table 1
Effect of sensitizer loading on $^1O_2$ generation.

Treatment	RB adsorbed (mg/cm^2)	R^1O_2 (x 10^{-7} M s^{-1})
1000-fold diluted stock	0.082	*ND
50-fold diluted stock	0.26	0.232
10-fold diluted	2	0.62
Undiluted stock (10 g RB in 150 g of gel)	9.4	3.32

* ND: Not detectable as there was no observable difference from blank.

CRediT authorship contribution statement

Michael Oluwatoyin Sunday: Investigation, Formal analysis, Writing - original draft. **Hiroshi Sakugawa:** Resources, Supervision, Writing - review & editing.

Declaration of competing interest

The authors declare that they have no known competing financial interests or personal relationships that could have appeared to influence the work reported in this paper.

Acknowledgment

We are grateful to Yokota Kogyo Shokai Co. Inc., Hiroshima, Japan for providing research funding for this study. We also appreciate Prof. Kazuhiko Takeda of the Graduate School of Biosphere Science, Hiroshima University, for the advice rendered during this study.

Appendix A. Supplementary data

Supplementary data to this article can be found online at https://doi.org/10.1016/j.scitotenv.2020.141186.

References

Aebisher, D., Zamadar, M., Mahendran, A., Ghosh, G., McEntee, C., Greer, A., 2010. Fiber-optic singlet oxygen [1O2 (1Δg)] generator device serving as a point selective sterilizer. Photochem. Photobiol. 86, 890–894.

Banks, J.G., Board, R.G., Carter, J., Dodge, A.D., 1985. The cytotoxic and photodynamic inactivation of micro-organisms by Rose Bengal. J. Appl. Bacteriol. 58, 391–400.

Bartusik, D., Aebisher, D., Lyons, A.M., Greer, A., 2012a. Bacteria inactivation by a singlet oxygen bubbler. Identifying factors controlling the toxicity of $^1O_2$ bubbles. Environ. Sci. Technol. 46 (21), 12098–12104.

Bartusik, D., Aebisher, D., Ghafari, B., Lyons, A.M., Greer, A., 2012b. Generating $^1O_2$ bubbles: a new mechanism for gas-liquid oxidations in water. Langmuir 38, 3053–3060.

Blacha-Grzechnik, A., Drewniak, A., Walczak, K.Z., Szindler, M., Ledwon, P., 2020. Efficient generation of singlet oxygen by perylene diimide photosensitizers covalently bound to conjugate polymers. J. Photochem. & Photobiol. A: Chemistry 388, 112161.

Carpenter, B.L., Scholle, F., Sadeghifar, H., Francis, A.J., Boltersdorf, J., Weare, W.W., Argyropoulos, D.S., Maggard, P.A., Ghiladi, R.A., 2015. Synthesis, characterization and antimicrobial efficacy of photomicrobicidal cellulose paper. Biomacromolecules 16, 2484–2492.

Costa, L., Faustino, M.A.F., Neves, M.G., Cunha, A., Almeida, A., 2012. Photodynamic inactivation of mammalian viruses and bacteriophages. Viruses 4, 1034–1074.

Crosley, D.R., Araps, C.J., Doyle-Eisele, M., Mcdonald, J.D., 2017. Gas-phase photolytic production of hydroxyl radicals in an ultraviolet purifier for air and surfaces. J. of air & waste mgt. assoc. 67, 231–240.

Dahl, T.A., Midden, W.R., Hartman, P.E., 1987. Pure $^1O_2$ cytotoxicity for bacteria. Photochem. Photobiol. 46, 345–352.

Dahl, T.A., Midden, W.R., Neckers, D.C., 1988. Comparison of photodynamic action by Rose Bengal in gram-positive and gram-negative bacteria. Photochem. Photobiol. 48, 607–612.

van Doremalen, N., Bushmaker, T., Morris, D.H., Holbrook, M.G., Gamble, A., Williamson, B.N., Tamin, A., Harcourt, J.L., Thornburg, N.J., Gerber, S.I., Lloyd-Smith, J.O., de Wit, E., Munster, V.J., 2020. Aerosol and surface stability of SARS-CoV-2 as compared with SARS-CoV-1. N. Engl. J. Med. 382, 16.

Eickmann, M., Gravemann, U., Handke, W., Tolksdorf, F., Reichenberg, S., Muller, T.H., Seltsam, A., 2018. Inactivation of Ebola virus and Middle East respiratory syndrome coronavirus in platelet concentrates and plasma by ultraviolet C light and methylene blue plus visible light, respectively. Transfusion 58, 2202–2207.

Felgenträger, A., Maisch, T., Späth, A., Schröder, J.A., Bäumler, W., 2014. $^1O_2$ generation in porphyrin-doped polymeric surface coating enables antimicrobial effects of Staphylococcus aureus. Phys. Chem. Chem. Phys. 2014 (16), 20598–20607.

Grandbois, M., Latch, D.E., Mcneill, K., 2008. Microheterogeneous concentrations of singlet oxygen in natural organic matter isolate solutions. Environ. Sci. Technol. 42, 9184–9190.

Haag, W.R., Hoigne, J.r., Gassman, E., Braun, A.M., 1984. Singlet oxygen in surface waters — part I: Furfuryl alcohol as a trapping agent. Chemosphere 13 (5), 631–640.

Hamblin, M.R., Hasan, T., 2004. Photodynamic therapy: a new antimicrobial approach to infectious disease? Photochem. Photobiol. Sci. 3, 436–450.

Hettegger, H., Gorfer, M., Sortino, S., Fraix, A., Bandian, D., Rohrer, C., Harreither, W., Potthast, A., Rosenau, T., 2015. Synthesis, characterization and photo-bactericidal activity of silanized xanthene-modified bacteria cellulose membranes. Cellulose 2015 (22), 3291–3304.

Huang, Q., Fu, W.-L., Chen, B., Huang, J.-F., Zhang, X., Xue, Q., 2004. Inactivation of dengue virus by methylene blue/narrow bandwidth light system. J. Photochem. Photobiol. B Biol. 2004 (77), 39–43.

Kim, H., Kim, W., MacKeyev, Y., Lee, G.-S., Kim, H.-J., Tashikawa, T., Hong, S., Lee, S., Kim, J., Wilson, L.J., Majima, T., Alvarez, P.J.J., Choi, W., Lee, J., 2012. Selective oxidative degradation of organic pollutants by singlet oxygen-mediated photosensitization: tin porphyrin versus C60 aminofullerene systems. Environ. Sci. Technol. 46, 9606–9613.

Kim, J., Lee, H., Lee, J.-Y., Park, K.-H., Kim, W., Lee, J.H., Kang, H.-J., Hong, S.W., Park, H.-J., Lee, S., Lee, J.-H., Park, H.-D., Kim, J.Y., Jeong, Y.W., Lee, J., 2020. Photosensitized production of singlet oxygen via C60 fullerene covalently attached to functionalized silica-coated stainless-steel mesh: remote bacterial and viral inactivation. Appl. Catal. B Environ. 270, 118862.

Latch, D.E., McNeill, K., 2006. Micorheterogeneity of singlet oxygen distributions in irradiated humic acid solutions. Science 311, 1743–1747.

Latch, D.E., Stender, B.L., Packer, J.L., Arnold, W.A., McNeill, K., 2003. Photochemical fate of pharmaceuticals in the environment: cimetidine and ranitidine. Environ. Sci. Technol. 37 (15), 3342–3350.

Lenard, J., Rabson, A., Vanderoef, R., 1993. Photodynamic inactivation of infectivity of human immunodeficiency virus and other enveloped viruses using hypericin and rose bengal: inhibition of fusion and synctia formation. Proc. Natl. Acad. Sci. 90, 158–162.

Lindig, B.A., Rodgers, M.A.J., Schaap, A.P., 1980. Determination of the lifetime of singlet oxygen in water-d2 using 9,10-anthracenedipropionic acid, a water-soluble probe. J. Am. Chem. Soc. 02 (17), 5590–5593.

Liu, N., Sun, G., 2011. Production of reactive oxygen species by photoactive anthraquinone compounds and their applications in wastewater treatment. Ind. Eng. Chem. Res. 50, 5326–5333.

Liu, Y., Qin, R., Zaat, S.A.J., Breukink, E., Heger, M., 2015. Antibacterial photodynamic therapy: overview of a promising approach to fight antibiotic-resistant bacterial infections. J. Clinical and Trans. Res. 1 (3), 140–167.

Masaoka, Y., Tagawa, M., Takao, S., 2013. Air Purification System (Japanese Patent 424167, Japan Patent office, December 6, 2013).

Nitzan, Y., Dror, R., Ladan, H., Malik, Z., Kimel, S., Gottfried, V., 1995. Structure-activity relationship of porphines for photoinactivation of bacteria. Photochem. Photobiol. 1995 (62), 342–347.

Rodgers, M.A.J., Snowden, P.T., 1982. Lifetime of oxygen (O2(1.DELTA.g)) in liquid water as determined by time-resolved infrared luminescence measurements. J. Am. Chem. Soc. 104 (20), 5541–5543.

Schagen, F.H.E., Moor, A.C.E., Cheong, S.C., Cramer, S.J., van Ormondt, H., van der Eb, A.J., Dubbelman, T.M.A.R., Hoeben, R.C., 1999. Photodynamic treatment of adenoviral vectors with visible light: an easy and convenient method for viral inactivation. Gene Ther. 1999 (6), 873–881.

Schweitzer, C., Schmidt, R., 2003. Physical mechanism of generation and deactivation of singlet oxygen. Chem. Rev. 103, 1685–1758.

Turner, G.S., Kaplan, C., 1968. Photoinactivation of vaccinia virus with rose bengal. J. Gen. Virol. 3, 433–443.

Usacheva, M.N., Teichert, M.C., Biel, M.A., 2001. Comparison of the methylene blue and toluidine blue photobactericidal efficacy against gram-positive and gram-negative microorganisms. Lasers Surg. Med. 29, 165–173.

Villen, L., Manjon, F., Garcia-Fresnadillo, D., Orellana, G., 2006. Solar water disinfection by photocatalytic singlet oxygen production in heterogeneous medium. Appl. Catal. B Environ. 69, 1–9.

Wainwright, M., Phoenix, D.A., Laycock, S.L., Wareing, D.R., Wright, P.A., 1998. Photobactericidal activity of phenothiazinium dyes against methicillin-resistant strains of Staphylococcus aureus. FEMS Microbiol. Lett. 160, 177–181.

Wilkinson, F., Brummer, L., 1981. Rate constants for the decay and reactions of the lowest electronically excited singlet-state of molecular oxygen in solutions. J. Phys. Chem. Ref. Data 10, 809–1000.

Wilkinson, J.F., Helman, P., Ross, A., 1992. Quantum yields for the photosensitized formation of the lowest electronically excited singlet state of molecular oxygen in solution. J. Phys. Chem. Ref. Data 22, 1–126.

Wong, T.-W., Huang, H.-J., Wang, Y.-F., Lee, Y.-P., Huang, C.-C., Yu, C.-K., 2010. Methylene bluemediated photodynamic inactivation as a novel disinfectant of enterovirus 71. J. Antimicrob. Chemother. 65, 2176–2182.

Xie, X., Zhang, Z., Hu, Y., Cheng, H.A., 2018. A mechanistic kinetic model for singlet oxygen mediated self-sensitized photo-oxidation of organic pollutants in water. Chem. Eng. J. 334, 1242–1251.

Zamadar, M., Aebisher, D., Greer, A., 2009. $^1O_2$ delivery through the porous cap of a hollow-core fiber optic device. J. Phys. Chem. B 113, 15803–15806.

Zhao, Y., Liu, Y., Xu, Q., Barahman, M., Bartusik, D., Greer, A., Lyons, A.M., 2014. $^1O_2$ generation on porous superhydrophobic surfaces: effect of gas flow and sensitizer wetting on trapping efficiency. J. Phys. Chem. A 118, 10364–10371.

Zhong, L., Haghighat, F., 2015. Photocatalytic air cleaners and materials technologies – abilities and limitations. Build. Environ. 9, 191–203.